CrossMark

ORIGINAL PAPER

Effects of various nanomaterials on the properties of starch/poly(vinyl alcohol) composite films formed by blow extrusion process

Wentao Wang[1] · Hui Zhang[1] · Yangyong Dai[1] · Hanxue Hou[1] · Haizhou Dong[1]

Abstract Effects of various nanomaterials on the physical and mechanical properties of hydroxypropyl distarch phosphate/poly(vinyl alcohol) (starch/PVA) composite films fabricated by blow extrusion were investigated. The starch/PVA nanocomposite films were studied by differential scanning calorimetry (DSC), thermogravimetric analysis (TGA/DTG), FTIR, and scanning electron microscope (SEM). The nanocomposite films containing nano-$CaCO_3$ and organically modified montmorillonite (OMMT) showed the lowest and highest tensile strengths of 3.72 and 7.04 MPa, respectively. The film containing natural montmorillonite (MMT) exhibited the lowest elongation-at-break of 118.73 %. The film with OMMT exhibited the lowest water vapor permeability of 4.12×10^{-10} g m^{-1} s^{-1} Pa^{-1}. Addition of nano-TiO_2 to starch/PVA films resulted in a significant decrease in ΔE^* (increased clearness). Differential scanning calorimetry (DSC) indicated that the nanocomposite films exhibited higher glass transition temperatures (T_g) and lower melting enthalpy compared to the control film. Adding MMT and OMMT to starch/PVA blends increased the thermal stabilities of the films according to the TGA/DTG analysis. Agglomeration of particles was observed in the starch/PVA composite films containing nano-$CaCO_3$ and nano-TiO_2 while nano-SiO_2 and MMT dispersed well in the matrix. On the whole, OMMT was more compatible with starch/PVA blends and served as a better nanomaterial to prepare starch/PVA nanocomposite films which was superior to that of the other four nanomaterials.

Keywords Starch · Poly(vinyl alcohol) · Nanocomposite · Film blowing · Properties

Introduction

A growing public concern for the harmful effects of non-degradable plastic films on the environment has stimulated increasing research on biodegradable films as alternatives to conventional petroleum-based films [1, 2]. Starch, a cheap, renewable, and biodegradable material, has been widely studied to prepare biodegradable films. However, pure starch films exhibit some severe limitations such as poor mechanical properties and high moisture sensitivity [3]. To overcome these drawbacks, starch has often been blended with other biodegradable synthetic polymers, such as poly(lactic acid) (PLA), poly(ε-caprolactone) (PCL), and PVA, which show promise in food packaging applications.

Starch/PVA composite films are one of the most popular biodegradable plastics in packaging and agricultural applications [4–6]. Starch and PVA are polar substances that contain many hydroxyl groups (–OH). These hydroxyl groups tend to form inter-molecular and intra-molecular hydrogen bonds and improve the integrity of starch/PVA blends [7]. Many approaches have been designed to further improve the moisture barrier and mechanical properties of starch/PVA blends, i.e. acid modification and plasma treatment [8], adding cross-linking agents [9], blending plasticizers, such as the mixture of glycerol and urea [10], or adding nanoparticles [11–13].

Of these methods, biodegradable nanocomposites have attracted much attention because of their good moisture

✉ Haizhou Dong
hzhdong28@126.com

Hanxue Hou
hhx@sdau.edu.cn

1 Department of Food Science and Engineering, Shandong Agricultural University, Tai'an 271018, People's Republic of China

barrier and mechanical properties [14]. Biodegradable starch-based nanocomposites have been prepared with organic or inorganic nanomaterials. Tang et al. [3] reported that nano-SiO₂ could improve the physical properties of starch/PVA films fabricated by solution casting. Majdza-deh-Ardakani et al. [15] reported that the mechanical properties of starch/PVA/clay nanocomposites containing OMMT were better than those of nanocomposites containing MMT. Sreekumar et al. [16] studied the effects of nano-titanium dioxide (TiO₂) on the mechanical properties of 1:1 starch/PVA composites. The results showed an increase in the tensile properties and a lower percentage of elongation- and energy-at-break particularly at higher content of nano-TiO₂. Yang et al. [17] prepared oxidized starch/PVA/exfoliated α-zirconium phosphate (α-ZrP) composites with a solution casting method. α-ZrP exhibited considerable advantages over clay, i.e. a much higher purity and surface energy, as well as easy intercalation and exfoliation [7].

The surface properties, structure, and interaction mechanism with the starch matrix depend on the nanomaterial [18–20]. The physico-chemical properties of starch-based nanocomposites are not only affected by starch sources but also by the film-forming process. Thus, the results from different research groups could not be easily compared to determine the best nanomaterial for starch-based nanocomposites. To the best of our knowledge, little information is available on comparisons of the starch/PVA composite films with various nanomaterials.

The high productivity and efficiency of extrusion film blowing in a laboratory setting verge on industrial production levels. However, extrusion film blowing has received less attention than solution casting for starch-based nanocomposites [21, 22]. In this study, the starch/PVA nanocomposite films were prepared by extrusion blowing. The starch used in this experiment was hydroxypropyl distarch phosphate, which showed good film-forming ability [23]. Nano-SiO₂, nano-TiO₂, nano-CaCO₃, MMT, and OMMT were used to improve the properties of starch/PVA composite films. The structure and physico-chemical properties of starch/PVA nanocomposite films were investigated.

Experimental

Materials

Hydroxypropyl distarch phosphate (HP-CF T0278) was purchased from Puluoxing Starch Co. (Hangzhou, China). Poly(viny alcohol) (PVA) with polymerization degree of 1700, alcoholysis degree of 99.0 %, and <0.6 % ash was obtained from Sinopec Sichuan Vinylon Works (Chongqing, China). Hydrophobic nano-SiO₂ (JY100-01, particle size ≤25 nm, specific surface area: 150–190 m²/g) was

obtained from Anhui Jingye Nanotechndogy Co. (Anhui, China). Nano-TiO₂ (average particle size: 5 nm, specific surface area: 90–110 m²/g) was obtained from Hangzhou Wanjing New Material Co. (Hangzhou, China). Nano-CaCO₃ (SHENGKE-206, average particle size: 65 nm, specific surface area: 22–28 m²/g) was obtained from Shandong Haize Nanomaterials Co. (Shandong, China). Natural MMT (average particle size: 8.66 μm) was obtained from Shandong Shouguang Zhonglian Fine montmorillonite Co. (Shouguang, China). OMMT (organically modified montmorillonite with octadecyl dimethyl benzyl ammonium as cation, average particle size: 18.31 μm) was obtained from Zhejiang Fenghong Co. (Zhejiang, China). Glycerol was obtained from Chemical Reagent Co. (Tianjin, China).

Compounding

Starch (1.7 kg), PVA (0.3 kg), glycerol (37.5 % of starch/PVA mass), and the nanomaterials (10 % of starch/PVA mass) were thoroughly blended in a mixer (SHR50A, Zhangjiagang, China) at room temperature for 15 min. The mixtures were stored in polyethylene bags at room temperature overnight to equilibrate all components. The mixtures were extruded at 90 °C in zone I and at 130 °C in zone II of the barrel in a laboratory-scale twin screw extruder (ZLYJ1014, Laiwu, China) at a screw speed of 60 rpm. The extrudates were cut into pellets and conditioned for at least 72 h at 23 ± 2 °C and 53 % relative humidity (Mg(NO₃)₂ saturated solution). They were then ground for film blowing.

Film blowing

Film blowing was conducted with a single-screw extruder (ZLYJ112, Laiwu, China) with a screw compression ratio of 3:1, diameter of 35 mm, length of 25D, and four individually controlled temperature zones. The extruder was equipped with a conventional temperature-controlled film-blowing die with a diameter of 60 mm and a film-blowing tower with a calendaring nip and haul-off rolls. The temperatures in the barrel and die were maintained at 55, 135, 145, 150, and 140 °C from feed inlet to die. In order to conveniently compare the properties of the composite films, the blow-up ratio and haul-off ratio in this study were carefully kept at 4:1 and 2:1, respectively. Figure 1 shows the continuous and stable preparation of starch/PVA nanocomposite films by film blowing.

Mechanical properties

The mechanical properties of the films were determined with a TA-XT2i texture analyzer (Stable Micro System, UK) according to ASTM D882-02. All tested films were

Fig. 1 Continuous and stable film blowing of starch/PVA nanocomposite films

cut into 15 mm wide and 120 mm long strips with a sharp knife and then conditioned at 23 ± 2 °C and 53 % relative humidity for 7 days prior to measurement. The initial distance between the grips was 50 mm. The thickness of the films was measured by a digital micrometer caliper (0–25 mm, 0.001 mm, Guilin, China) at three random positions on the films. The average thickness of the films was 76, 72, 81, 74, 84, and 75 μm for blank control, nano-$CaCO_3$, nano-SiO_2, nano-TiO_2, MMT and OMMT nanocomposites, respectively. The crosshead speed was set at 1 mm/s. Each test was run six replicates. The tensile strength (TS, MPa) and elongation-at-break (*E*, %) were determined based on previous reports [3, 24].

Water vapor permeability (WVP)

The water vapor permeability (WVP) of the films was analyzed according to ASTM E96-95 with some modifications using an Automatic Water Vapor Permeability Tester (PERME™ W3/030, Jinan, China). The films were cut into circles (an area of 33.00 cm^2) with a special sampler and equilibrated for 7 days in a desiccator at 23 °C and 53 % relative humidity prior to the test. The thicknesses of films were measured five times with a digital micrometer caliper (0–25 mm, 0.001 mm, Guilin, China). The test was then conducted at 38 °C and 90 % relative humidity. The WVP of each sample was averaged from three separate tests.

Color

The color of the composite films was determined with a Chroma Meter CR-400 colorimeter (Konica Minolta, Japan). The composite films were placed on the standard white plate at different locations, and each film was measured five times. The L^* a^* b^* color system was used, where L^* is 0 for black and 100 for white; a^* indicates red (+) to green (−), and b^* indicates yellow (+) to blue (−). The colorimeter was calibrated with a standard white plate ($L^* = 87.7$, $a^* = +0.3158$, $b^* = +0.3225$).

Differential scanning calorimetry (DSC)

Differential scanning calorimetry (DSC) measurements of the films were carried out in a nitrogen atmosphere on a DSC 200PC (Netzsch Scientific Instruments, Germany) instrument from −10 to 250 °C with a heating rate of 10 °C/min. All films were conditioned for 3 days at 23 ± 2 °C and 53 % relative humidity in desiccators prior to the test. Aluminum pans containing 5–10 mg of films were hermetically sealed with the DSC sample press. An empty, hermetically sealed aluminum pan was used as a reference. Each sample was scanned three times.

Thermogravimetric analysis (TGA)

Thermogravimetric analysis (TGA) was performed with a DTG-60AH at a heating rate of 15 °C/min from room temperature to 800 °C. The samples (5–10 mg) were analyzed in a nitrogen atmosphere with a flow rate of 100 mL/min.

FTIR analysis

The Fourier transform infrared (FTIR) spectra of the films were measured with a Thermo Fisher Scientific (USA) Nexus 670 spectrometer attached to the Smart iTR diamond ATR accessory from 4000 to 600 cm^{-1}. Thirty-two scans were accumulated, and the scanning resolution was 4 cm^{-1}. The film was mounted directly in the sample holder [25].

Fig. 2 Mechanical properties of starch/PVA films with various nanomaterials: **a** longitudinal and transversal tensile strength and **b** longitudinal and transversal elongation-at-break. *TS* tensile strength, *E* elongation-at-break, *BC* blank control, *MMT* montmorillonite, *OMMT* organically modified montmorillonite
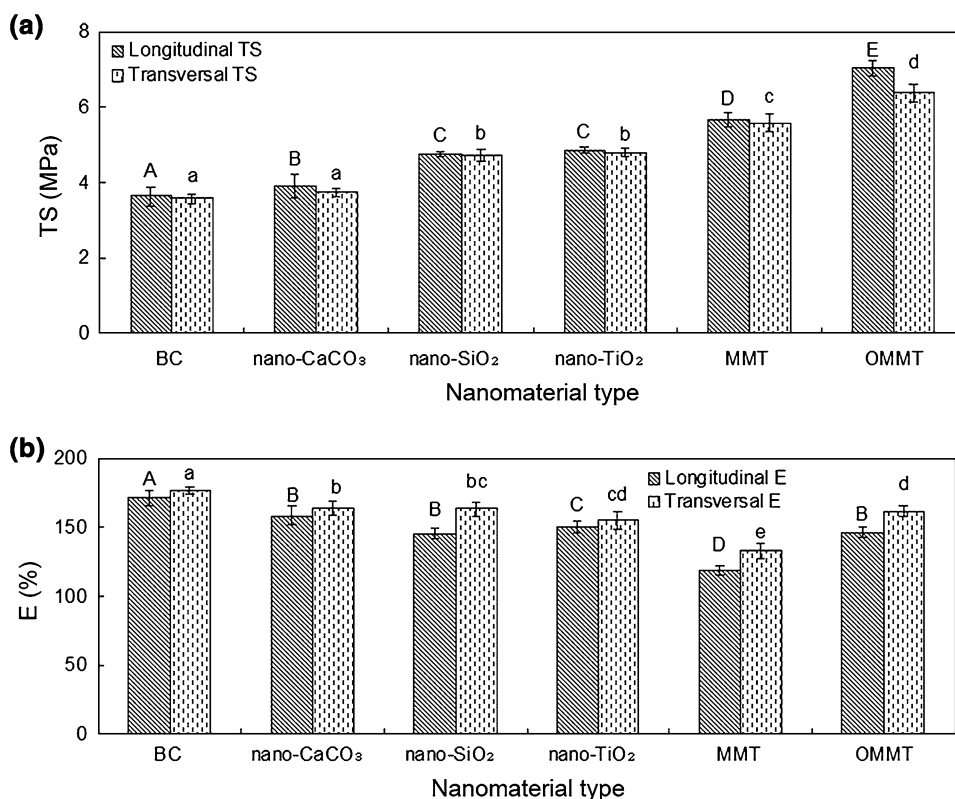
Morphology of the films

The surface morphology of the films was observed with a Quanta FEG 250 scanning electron microscope (SEM) (FEI, USA) operated at voltage of 5.0 kV. The film samples were mounted on a bronze stub and sputter-coated with a layer of gold prior to taking picture.

Statistical analysis

The statistical differences in the film functional properties between samples were analyzed with an analysis of variance (ANOVA). Duncan's multiple range test ($P < 0.05$) was used to detect differences among the mean values of film properties. A statistical analysis was conducted with SPSS (Version 17.0, Chicago, USA) software.

Results and discussion

Mechanical properties of starch composite films

The mechanical properties of starch/PVA films were measured in longitudinal and transverse directions. The direction parallel to the extruder is usually called the longitudinal direction (Fig. 1), while the direction perpendicular of the extruder is named the transversal direction. Figure 2

illustrates the tensile strength (TS, MPa) and elongation-at-break (*E*, %) of various composite films containing 10 % nanomaterials.

Figure 2 shows that the addition of various nanomaterials to starch/PVA blends could improve the tensile strength but lowering the elongation-at-break of the films. Compared with the control film, the tensile strength of nanocomposite films increased by 5–98 % (Fig. 2a). The nanocomposite films containing nano-CaCO$_3$ and OMMT showed the lowest and highest tensile strengths of 3.72 and 7.04 MPa, respectively. Nano-SiO$_2$ and nano-TiO$_2$ moderately reinforced the starch/PVA composite films. The interaction mechanism with polymers was specific to the nanomaterials [19, 26, 27]. Addition of nano-SiO$_2$, nano-TiO$_2$, and nano-CaCO$_3$ to starch/PVA blends improved the interfacial adhesion through intermolecular interactions between nanoparticles and starch or nanoparticles and PVA which increased the tensile strength of starch/PVA nanocomposite films [28–30]. MMT and OMMT improved the mechanical properties of polymers by forming intercalated or exfoliated nanocomposites [12, 21]. The highest tensile strength of starch/PVA/OMMT composite films indicated that hydroxypropyl distarch phosphate was compatible with OMMT [21]. The tensile strength of starch/PVA composite films in this study was generally lower than previously reported [19], which was possibly due to the different starches used and preparation conditions of the films.

Fig. 3 Water vapor permeability (WVP) of starch/PVA films with various nanomaterials. *BC* blank control, *MMT* montmorillonite, *OMMT* organically modified montmorillonite
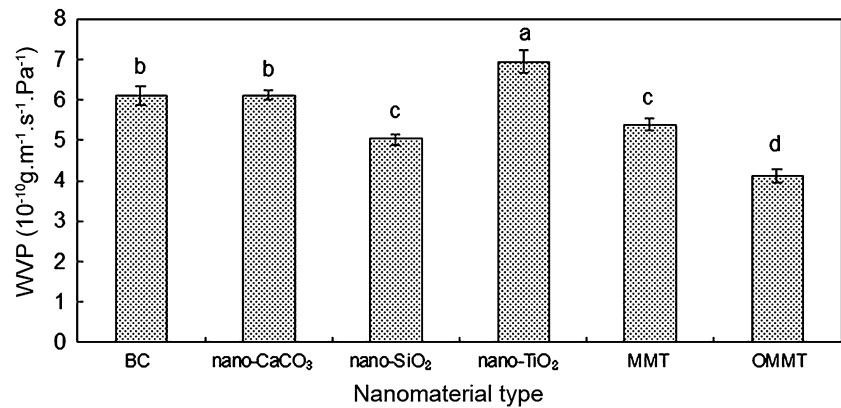
Table 1 Color parameters (*L**, *a**, *b**) and total color differences (Δ*E**) of starch/PVA films with various nanomaterials

Nanomaterial type	L^*	a^*	b^*	ΔE^*
Blank control	$91.10 \pm 0.88ab$	$-0.31 \pm 0.024c$	$5.52 \pm 0.39d$	$6.30 \pm 0.19d$
Nano-CaCO$_3$	$90.28 \pm 0.72b$	$-0.40 \pm 0.035d$	$6.31 \pm 0.33c$	$6.59 \pm 0.081cd$
Nano-SiO$_2$	$88.57 \pm 0.97c$	$-0.26 \pm 0.017b$	$7.87 \pm 0.61b$	$7.68 \pm 0.48b$
Nano-TiO$_2$	$88.33 \pm 0.25c$	$-0.39 \pm 0.021d$	$5.54 \pm 0.17d$	$5.31 \pm 0.17e$
MMT	$88.01 \pm 0.62c$	$-0.21 \pm 0.021a$	$8.84 \pm 0.39a$	$8.56 \pm 0.36a$
OMMT	$91.81 \pm 0.76a$	$-0.33 \pm 0.018c$	$5.78 \pm 0.50cd$	$6.91 \pm 0.075c$

Different lowercase letters in the same column for different nanomaterial types indicated significant differences ($P < 0.05$). Data shown in mean $\pm$ standard deviation ($n = 5$)

All films showed good elongation-at-break, though this parameter decreased from 163.80 to 118.73 % with the addition of nanomaterials (Fig. 2b). This result agreed with previous reports which suggested that the dispersion of nanomaterials in the polymer reduced the tensile ductility and improved the strength compared to neat polymer [21, 31].

Figure 2 also shows the longitudinal and transversal properties of starch/PVA nanocomposite films. The tensile strength and elongation-at-break were high and low in the longitudinal direction; by contrast, the tensile strength and elongation-at-break were low and high in the transversal direction of the films. This was due to the combination effects of blowing up and hauling off ratios of nanocomposite films. Thunwall et al. [22] reported the tensile strength of hydroxypropylated and oxidized potato starch film was greater in the longitudinal direction than in the transversal direction. Ghaneh-Fard [32] studied the effects of the blow-up ratio and haul-off ratio on the molecular orientation and mechanical properties of polyethylene films. The author found that the modulus in the transversal direction considerably increased as the haul-off ratio increased at low blow-up ratios.

Water vapor permeability (WVP) of the starch composite films

The effects of different nanomaterials on the WVP are shown in Fig. 3. The values of WVP ranged from 4.12×10^{-12} to 6.94×10^{-12} g m^{-1} s^{-1} Pa^{-1} for the starch/PVA nanocomposite films. The WVPs of starch/PVA composite films containing nano-SiO$_2$ and OMMT were lower than those of composite films containing nano-TiO$_2$ and nano-CaCO$_3$. Both the nano-SiO$_2$ and OMMT used in this study were organically modified to be more hydrophobic. The similar hydrophobicity of the hydroxypropyl distarch phosphate/PVA blend and nano-SiO$_2$ or OMMT enhanced the intermolecular interactions and decreased the molecular mobility. The good dispersion of nano-SiO$_2$ and OMMT increased the water molecule migration pathways and then limited the permeability of the film [33]. However, nano-TiO$_2$ and nano-CaCO$_3$ may not interact well with the hydroxypropyl distarch phosphate/PVA matrix due to their hydrophilic properties.

Color

The film color is an important factor in terms of consumer acceptance for a product. The values of L^*, a^*, b^*, and ΔE^* are shown in Table 1. The control sample (without nanomaterials) showed a higher L^* value (lighter), a^* value (greenish), and lower ΔE^* (cleaner). The b^* value (yellowish) was the lowest compared with starch/PVA films containing nanomaterials. This finding indicated that starch/PVA blends could produce light greenish yellow films.

The surfaces of films containing MMT were dark greenish and opaque yellowish, which were indicated by the

Table 2 The effect of various nanomaterials on thermal properties of starch/PVA films

Composite film	T_g (°C)	T_m (°C)	ΔH (J/g)
Starch/PVA	44.7 ± 1.13a	171.0 ± 2.21c	112.4 ± 1.79d
Starch/PVA/nano-CaCO$_3$	55.8 ± 2.76c	178.1 ± 8.96d	89.71 ± 2.37c
Starch/PVA/nano-SiO$_2$	61.8 ± 2.31d	168.2 ± 2.44b	78.34 ± 1.65a
Starch/PVA/nano-TiO$_2$	80.7 ± 3.17e	162.3 ± 3.53a	88.98 ± 3.78c
Starch/PVA/MMT	52.3 ± 2.60b	172.2 ± 6.36c	89.66 ± 2.53c
Starch/PVA/OMMT	55.7 ± 1.78c	168.6 ± 2.92b	81.23 ± 2.45b

T_g glass transition temperature, T_m melting temperature, ΔH melting enthalpy

Different lowercase letters in the same column for different nanomaterial types indicated significant differences ($P < 0.05$). Data shown in mean ± standard deviation ($n = 5$)

lowest $L*$ values (darkness), highest $a*$ value (greenish), highest $b*$ value (yellowish), and highest $\Delta E*$ (opaque) compared with other films. In contrast, the darkness of the films containing OMMT was significantly ($P < 0.05$) decreased (expressed as the $L*$ value). The greenish color of the films containing nano-CaCO$_3$ was significantly increased ($P < 0.05$) (expressed as $a*$ value). Unexpectedly, adding nano-TiO$_2$ to starch/PVA films resulted in a significant drop ($P < 0.05$) in $\Delta E*$ (increased clarity).

Differential scanning calorimeter (DSC)

DSC is a useful technology to determine the glass transition temperature (T_g), melting temperature (T_m), and enthalpy (ΔH) of polymer materials. The T_g, T_m, and ΔH of starch/PVA blends with various nanofillers are presented in Table 2. The T_g of all starch/PVA nanocomposite films increased compared to that of the starch/PVA film. The starch/PVA/nano-TiO$_2$ film had the highest T_g of 80.7 °C while the control film had the lowest T_g of 44.7 °C. The increase in T_g for the starch/PVA nanocomposite films may be attributed to the intermolecular interactions between the starch/PVA matrix and the nanoparticles which reduced the flexibility of the starch/PVA molecular chains. Previous studies also showed that addition of nanofillers increased the T_g of starch-based nanocomposites compared to the polymer matrix without nanofillers [34–36]. The difference of T_g and T_m among various starch/PVA nanocomposites may be due to the different dispersion state and inherent properties of various nanofillers.

The melting enthalpy (ΔH) for each film is also summarized in Table 2. The ΔH of the nanocompoiste films was significantly lower than that of the control film which indicated a reduced order of starch/PVA molecular arrangement. This reduction may be due to the presence of highly dispersed nanoparticles in the starch/PVA matrix which hindered the growth of microcrystalline polymer molecules

[34, 37]. There were new shoulder peaks on the melt endotherms for starch/PVA nanocomposite films which indicated that a new type of crystallinity was formed. The nanofillers might have acted as nucleating agents which induced the formation of new crystallinity.

Thermogravimetric analysis (TGA/DTG)

The thermogravimetric (TGA/DTG) curves of the starch/PVA films with various nanomaterials are presented in Fig. 4. The thermal decomposition process of the composite films showed three main stages. However, the effects of nanomaterial types on the thermogravimetric curves of the films differed remarkably, which implied the different decomposition mechanism of the starch/PVA films. The first weight loss occurred between 50 and 165 °C, which corresponded to vaporization of water [38]. The temperatures corresponding to maximum rate of mass loss for the films without nanomaterial and with nano-CaCO$_3$, nano-SiO$_2$, nano-TiO$_2$, MMT, and OMMT were observed at 96.71, 95.18, 96.72, 97.48, 99.81, and 101.35 °C, respectively. The results indicated that MMT and OMMT had slightly higher capability of delaying water vaporization than other nanomaterials.

The second weight loss was found approximately at temperature range of 228–420 °C, mainly related to the decomposition of the composite films (Fig. 4). The onset temperatures of decomposition of the films were 239.6, 228.6, 231.4, 254.3, 262.3, and 260.6 °C for blank control, nano-CaCO$_3$, nano-SiO$_2$, nano-TiO$_2$, MMT, and OMMT composites, respectively. The mass loss of the films without nanomaterial and with nano-CaCO$_3$, nano-SiO$_2$, nano-TiO$_2$, MMT, and OMMT for the second stage was 63.55, 53.64, 53.78, 56.10, 52.06, and 57.48 %, respectively. These results indicated that addition of the nanomaterials increased the thermal stability of the starch/PVA films to a certain extent. Similar results were reported in previous studies [14, 39]. Moreover, the DTG curves in Fig. 4a, b showed visible shoulder peaks at around 283 °C, which was most likely due to the decomposition of the glycerol-rich phase [38, 40]. The highest peaks in the DTG curves near 333 °C were probably associated with the degradation of the starch/PVA-rich phase [38]. In Fig. 4c, d, the shoulder peaks of DTG curves become much smaller, but they are still visible. However, in the case of Fig. 4e, f, no shoulder peak can be seen. This indicates that the extent of phase separation is in the order of blank control film, nano-CaCO$_3$ composite film > nano-SiO$_2$, nano-TiO$_2$ composite films > MMT, OMMT composite films. This result is in agreement with mechanical and water vapor properties of the starch/PVA nanocomposite films.

The third weight loss in the TGA curves (Fig. 4) may correspond to the decomposition of un-decomposed nanomaterials. The residual weight significantly differs among different nanocomposites. As shown in Fig. 4, the residual

Fig. 4 TGA/DTG curves of starch/PVA films: **a** without nanomaterials, **b** with nano-CaCO₃, **c** with nano-TiO₂, **d** with nano-SiO₂, **e** with MMT and **f** with OMMT. *MMT* montmorillonite, *OMMT* organically modified montmorillonite
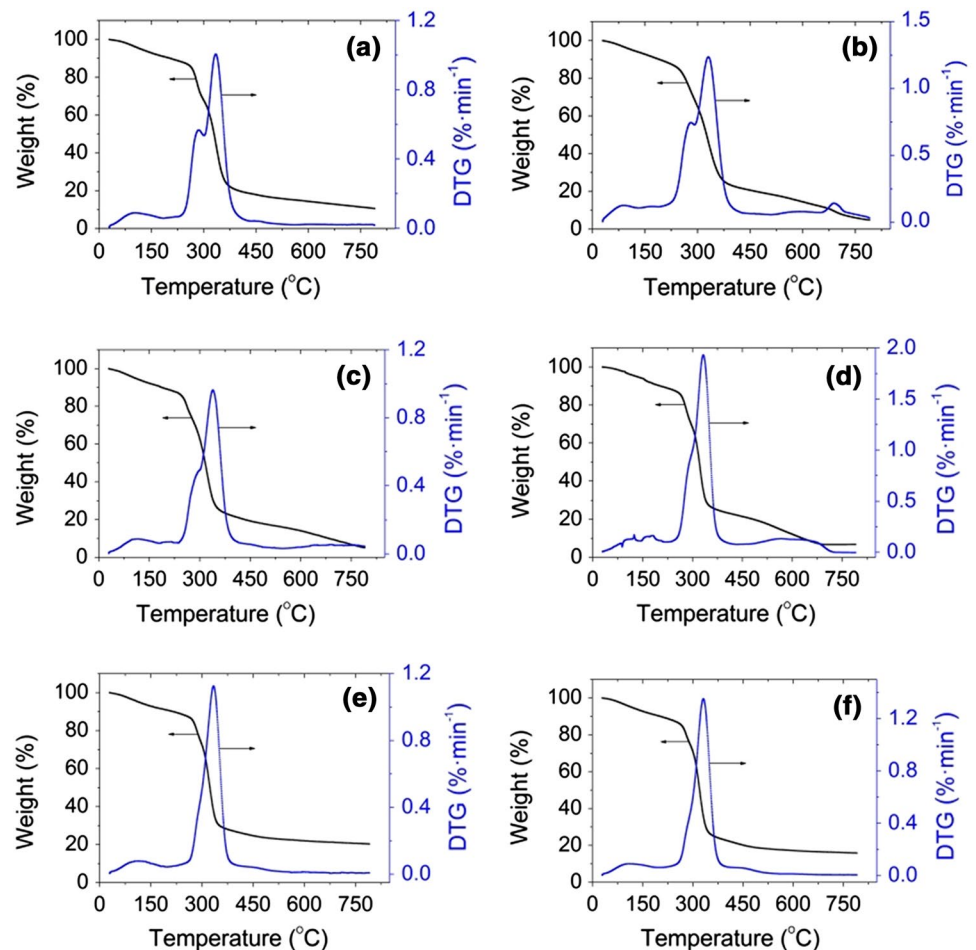

weight percentages at 650 °C for starch/PVA films without nanomaterial, with nano-CaCO₃, nano-SiO₂, nano-TiO₂, MMT, and OMMT were 12, 13, 11, 10, 21, and 19 %, respectively. The residual weight of the films also reflects that MMT and OMMT have significantly increased the thermal stability of starch/PVA films because of their ability to act as a heat barrier at high temperature [39]. In addition, the DTG curve in Fig. 4b shows an obvious peak at 689 °C, which is most likely due to the heating pyrolysis of CaCO₃ into CaO. Kisku et al. [41] reported that pure nano-CaCO₃ was decomposed and about 60 % residue was left at 680 °C.

FTIR analysis

FTIR is a useful tool to analyze the interactions between starch/PVA and nanomaterials or plasticizers. The FTIR spectra of starch/PVA films containing various nanomaterials are shown in Fig. 5.

The strong and wide absorption bands near 3346.0 cm⁻¹ in the spectra of nanocomposite films may be assigned to the characteristic absorption peak of the stretching vibration of –OH. Adding nanomaterials into starch/PVA films
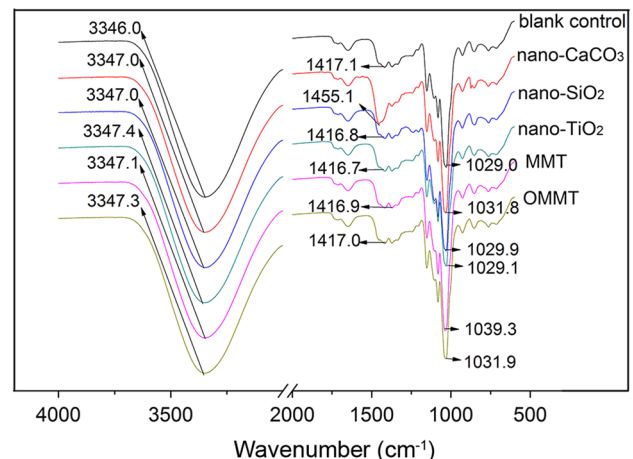
Fig. 5 FTIR spectra of starch/PVA films with various nanomaterials. *MMT* montmorillonite, *OMMT* organically modified montmorillonite

shifted the peaks to a higher wavenumber, which indicated that new hydrogen bonds were formed between the nanomaterials and starch/PVA blends [19].

The characteristic absorption peak near 1416.0 cm^{-1} was attributed to the stretching vibration of C–H. In the FTIR spectra of starch/PVA films containing nano-CaCO$_3$, the peak for C–H appeared at 1455.1 cm^{-1}, a much higher wavenumber than those of other nanocomposite films. According to the harmonic oscillator model, the peak frequency negatively correlates with the molecular interaction [42]. Thus, the intermolecular interaction in starch/PVA/nano-CaCO$_3$ films was much weaker than those of other nanocomposite films.

The absorption peaks near 1030.0 cm^{-1} were attributed to C–O bond stretching. These peaks could be used to evaluate the thermoplasticization process of polymers [43, 44]. The peak at 1029.0 cm^{-1} of the starch/PVA film was shifted to a higher wavenumber of the composite films containing nanomaterials. These changes resulted from the plasticization of glycerol in the film-forming process, which indicated that the nanomaterials restrained the thermoplasticization between glycerol and starch/PVA blends. Thus, the films showed weaker flexibility, i.e. decreased elongation-at-break.

Morphology of films

Figure 6 shows the SEM micrographs of starch/PVA films containing various nanomaterials. The surface of the control film appears more homogeneous and smoother than those of the starch/PVA nanocomposite films (Fig. 6a). Some agglomeration of particles is observed on the surfaces of starch/PVA composite films containing nano-CaCO$_3$ and nano-TiO$_2$ (Fig. 6b, c), which may result in a higher WVP and lower tensile strength of the films. The nano-SiO$_2$ and MMT dispersed well in the starch/PVA matrix (Fig. 6d, e). OMMT was well dispersed throughout the starch/PVA composite film, and an intercalated/exfoliated structure was obtained [45]. The six micrographs supported the determined mechanical properties and WVPs of the starch/PVA nanocomposite films. OMMT was the preferred choice to prepare starch/PVA nanocomposite films.

Conclusion

The extrusion blowing process was used to prepare starch/PVA nanocomposite films with various nanomaterials. The five nanomaterials significantly affected the properties of the films. The addition of nano-SiO$_2$ to starch/PVA film resulted in the lowest melting enthalpy of the nanocompoiste films. The composite film containing nano-CaCO$_3$
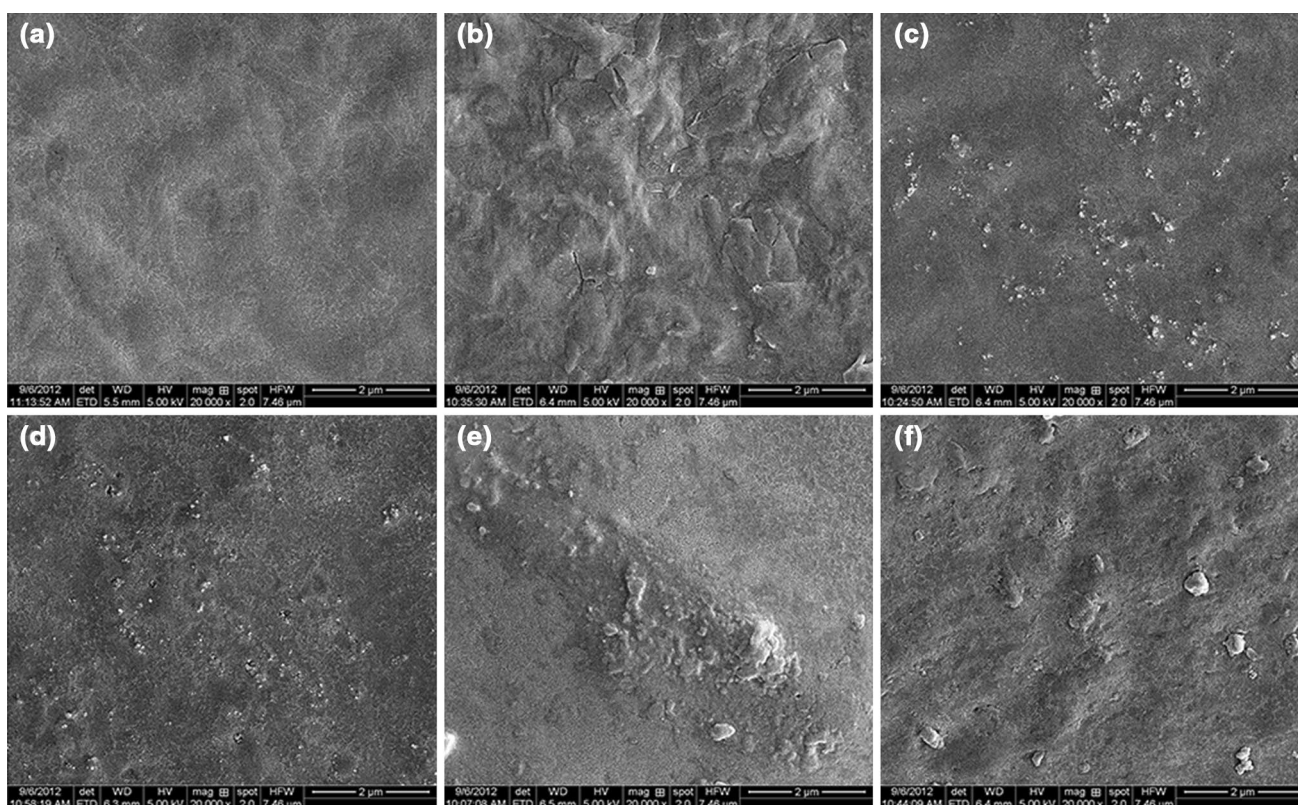
Fig. 6 SEM micrographs of starch/PVA films: **a** without nanomaterials, **b** with nano-CaCO$_3$, **c** with nano-TiO$_2$, **d** with nano-SiO$_2$, **e** with MMT and **f** with OMMT. *MMT* montmorillonite, *OMMT* organically modified montmorillonite

showed the highest melting temperature (178.1 °C) but the lowest tensile strength (3.72 MPa). The composite film containing nano-TiO$_2$ was significantly clearer but more permeable to water vapor (6.94×10^{-10} g m^{-1} s^{-1} Pa^{-1}). The addition of OMMT to starch/PVA film resulted in the highest tensile strength (7.04 MPa) and lowest permeability to water vapor (4.12×10^{-10} g m^{-1} s^{-1} Pa^{-1}). OMMT was well-dispersed throughout the starch/PVA matrix and was more suitable for fabrication of starch/PVA nanocomposite films as an intensifier than the other four nanomaterials.

References

1. Marcin M, Agnieszka W, Leszek, Moscicki (2009) In: Leon PBM, Janssen L Moscicki (eds) Biodegradable polymers and their practical utility. Wiley, New York

2. Wang SY, Ren JL, Li WY, Sun RC, Liu SJ (2014) Properties of polyvinyl alcohol/xylan composite films with citric acid. Carbohydr Polym 103:94–99

3. Tang SW, Zou P, Xiong HG, Tang HL (2008) Effect of nano-SiO$_2$ on the performance of starch/polyvinyl alcohol blend films. Carbohydr Polym 72:521–526

4. Follain N, Joly C, Dole P, Bliard C (2005) Properties of starch based blends. Part 2. Influence of polyvinyl alcohol addition and photocrosslinking on starch based materials mechanical properties. Carbohydr Polym 60:185–192

5. He YQ, Wang XR, Wu D, Gong QJ, Qiu HX, Liu Y, Wu T, Ma JK, Gao JP (2013) Biodegradable amylose films reinforced by graphene oxide and polyvinyl alcohol. Mater Chem Phys 142:1–11

6. Priya B, Gupta VK, Pathania D, Singha AS (2014) Synthesis, characterization and antibacterial activity of biodegradable starch/PVA composite films reinforced with cellulosic fibre. Carbohydr Polym 109:171–179

7. Tang XZ, Alavi S (2011) Recent advances in starch, polyvinyl alcohol based polymer blends, nanocomposites and their biodegradability. Carbohydr Polym 85:7–16

8. Yang SY, Liu CI, Wu JY, Kuo JC, Huang CY (2008) Improving the processing ability and mechanical strength of starch/poly(vinyl alcohol) blends through plasma and acid modification. Macromol Symp 272:150–155

9. Yoon S, Chough S, Park H (2007) Preparation of resistant starch/poly(vinyl alcohol) blend films with added plasticizer and crosslinking agents. J Appl Polym Sci 106:2485–2493

10. Zhou XY, Cu YF, Jia DM, Xie D (2009) Effect of a complex plasticizer on the structure and properties of the thermoplastic PVA/starch blends. Polym Plast Technol Eng 48:489–495

11. Azeredo HMC (2009) Nanocomposites for food packaging applications. Food Res Int 42:1240–1253

12. Chivrac F, Pollett E, Schmutz M (2008) New approach to elaborate exfoliated starch-based nanobiocomposites. Biomacromolecules 9:896–900

13. Jordan J, Jacob KI, Tannenbaum R, Sharaf MA, Jasiuk I (2005) Experimental trends in polymer nanocomposites-a review. Mater Sci Eng A 393:1–11

14. Xie FW, Pollet E, Halley PJ, Avérous L (2013) Starch-based nano-biocomposites. Prog Polym Sci 38:1590–1628

15. Majdzadeh AK, Nazari B (2010) Improving the mechanical properties of thermoplastic starch/poly(vinyl alcohol)/clay nanocomposites. Compos Sci Technol 70:1557–1563

16. Sreekumar PA, Al-Harthi MA, De SK (2012) Reinforcement of starch/polyvinyl alcohol blend using nano-titanium dioxide. J Compos Mater 46:3181–3187

17. Yang Y, Liu C, Chang PR, Chen Y, Anderson DP, Stumborg M (2010) Properties and structural characterization of oxidized starch/PVA/α-zirconium phosphate composites. J Appl Polym Sci 115:1089–1097

18. Chaichana E, Jongsomjit B, Praserthdam P (2007) Effect of nano-SiO$_2$ particle size on the formation of LLDPE/SiO$_2$ nanocomposite synthesized via the in situ polymerization with metallocene catalyst. Chem Eng Sci 62:899–905

19. Xiong HG, Tang SW, Tang HL, Zou P (2008) The structure and properties of a starch-based biodegradable film. Carbohydr Polym 71:263–268

20. Yu L, Dean K, Li L (2006) Polymer blends and composites from renewable resources. Prog Polym Sci 31:576–602

21. Gao W, Dong HZ, Hou HX, Zhang H (2012) Effects of clays with various hydrophilicities on properties of starch–clay nanocomposites by film blowing. Carbohydr Polym 88:321–328

22. Thunwall M, Kuthanova V, Boldizar A, Rigdahl M (2008) Film blowing of thermoplastic starch. Carbohydr Polym 71:583–590

23. Lafargue D, Pontoire B, Buléon A, Doublier JL, Lourdin D (2007) Structure and mechanical properties of hydroxypropylated starch films. Biomacromolecules 8:3950–3958

24. Yan QQ, Hou HX, Guo P, Dong HZ (2011) Effects of extrusion and glycerol content on properties of oxidized and acetylated corn starch-based films. Carbohydr Polym 87:707–712

25. Sudhamani SR, Prasad MS, Udaya Sankar K (2003) DSC and FTIR studies on Gellan and polyvinyl alcohol (PVA) blend films. Food Hydrocolloid 17:245–250

26. Cyras VP, Manfredi LB, Ton-That MT, Vazquez A (2008) Physical and mechanical properties of thermoplastic starch/montmorillonite nanocomposite films. Carbohydr Polym 73:55–63

27. Chen N, Wan C, Zhang Y, Zhang Y (2004) Effect of nano-CaCO$_3$ on mechanical properties of PVC and PVC/Blendex blend. Polym Test 23:169–174

28. Al-Turaif HA (2010) Effect of nano TiO$_2$ particle size on mechanical properties of cured epoxy resin. Prog Org Coat 69:241–246

29. Tang H, Xiong H, Tang S, Zou P (2009) A starch-based biodegradable film modified by nano silicon dioxide. J Appl Polym Sci 113:34–40

30. Gao Y, Liu L, Zhang Z (2009) Mechanical performance of nano-CaCO$_3$ filled polystyrene composites. Acta Mech Solida Sin 22:555–562

31. Lee JH, Jung D, Hong CE, Rhee KY, Advani SG (2005) Properties of polyethylene-layered silicate nanocomposites prepared by melt intercalation with a PP-g-MA compatibilizer. Compos Sci Technol 65:1996–2002

32. Ghaneh-Fard A (1999) Effects of film blowing conditions on molecular orientation and mechanical properties of polyethylene films. J Plast Film Sheet 15:194–218

33. Deborah LC, Julien B, Alain D (2010) Starch nanoparticles: a review. Biomacromolecules 11:1139–1153

34. Cao X, Chen Y, Chang PR, Huneault MA (2007) Preparation and properties of plasticized starch/multiwalled carbon nanotubes composites. J Appl Polym Sci 106:1431–1437

35. Chivrac F, Pollet E, Avérous L (2009) Progress in nano-biocomposites based on polysaccharides and nanoclays. Mater Sci Eng R Rep 67:1–17

36. Chang PR, Jian R, Yu J, Ma X (2010) Starch-based composites reinforced with novel chitin nanoparticles. Carbohydr Polym 80:420–425

37. Liu H, Chaudhary D, Yusa SI, Tadé MO (2011) Glycerol/starch/Na$^+$-montmorillonite nanocomposites: a XRD, FTIR, DSC and ^{1}H NMR study. Carbohydr Polym 83:1591–1597

38. García NL, Ribba L, Dufresne A, Aranguren MI, Goyanes S (2009) Physico-mechanical properties of biodegradable starch nanocomposites. Macromol Mater Eng 294:169–177

39. Ma X, Yu J, Wang N (2007) Production of thermoplastic starch/MMT-sorbitol nanocomposites by dual-melt extrusion processing. Macromol Mater Eng 292:723–728

40. Mu C, Guo J, Li X, Lin W, Li D (2012) Preparation and properties of dialdehyde carboxymethyl cellulose crosslinked gelatin edible films. Food Hydrocolloid 27:22–29

41. Kisku SK, Sarkar N, Dash S, Swain SK (2014) Preparation of starch/PVA/CaCO$_3$ nanobiocomposite films: study of fire retardant, thermal resistant, gas barrier and biodegradable properties. Polym Plast Technol 53:1664–1670

42. Pawlak A, Mucha M (2003) Thermogravimetric and FTIR studies of chitosan blends. Thermochim Acta 396:153–166

43. Fang JM, Fowler PA, Tomkinson J, Hill CAS (2002) The preparation and characterisation of a series of chemically modified potato starches. Carbohydr Polym 47:245–252

44. Zullo R, Iannace S (2009) The effects of different starch sources and plasticizers on film blowing of thermoplastic starch: correlation among process, elongational properties and macromolecular structure. Carbohydr Polym 77:376–383

45. Majdzadeh-Ardakani K, Navarchian AH, Sadeghi F (2010) Optimization of mechanical properties of thermoplastic starch/clay nanocomposites. Carbohydr Polym 79:547–554